Raman spectroscopic study of hydrogen ordered ice XIII and of its reversible phase transition to disordered ice V

ARTICLE *in* PHYSICAL CHEMISTRY CHEMICAL PHYSICS · AUGUST 2006

Impact Factor: 4.49 · DOI: 10.1039/b604360g · Source: PubMed

4 AUTHORS, INCLUDING:

Christoph Salzmann
University College London
69 PUBLICATIONS **1,697** CITATIONS
SEE PROFILE

Andreas Hallbrucker
University of Innsbruck
117 PUBLICATIONS **4,177** CITATIONS
SEE PROFILE

Raman spectroscopic study of hydrogen ordered ice XIII and of its reversible phase transition to disordered ice V

Christoph G. Salzmann,*[ab] Andreas Hallbrucker,[a] John L. Finney[c] and Erwin Mayer[a]

Received 29th March 2006, Accepted 16th May 2006
First published as an Advance Article on the web 1st June 2006
DOI: 10.1039/b604360g

Raman spectra of recovered ordered H_2O (D_2O) ice XIII doped with 0.01 M HCl (DCl) recorded *in vacuo* at 80 K are reported in the range 3600–200 cm^{-1}. The bands are assigned to the various types of modes on the basis of isotope ratios. On thermal cycling between 80 and 120 K, the reversible phase transition to disordered ice V is observed. The remarkable effect of HCl (DCl) on orientational ordering in ice V and its phase transition to ordered ice XIII, first reported in a powder neutron diffraction study of DCl doped D_2O ice V (C. G. Salzmann, P. G. Radaelli, A. Hallbrucker, E. Mayer, J. L. Finney, *Science*, 2006, **311**, 1758), is demonstrated by Raman spectroscopy and discussed. The dopants KOH and HF have only a minor effect on hydrogen ordering in ice V, as shown by the Raman spectra.

Introduction

Thermodynamically, the hydrogen disordered phases of ice should, on cooling, transform *via* hydrogen ordering into new, thermodynamically more stable phases, with zero entropy at 0 K.[1] The structures of these lowest energy states are important for differentiating between various potential functions used in simulations of water and aqueous systems. The basic obstacle in achieving these phase transitions is the slowing down of the reorientation of water molecules with decreasing temperature and a consequent freezing-in of disorder. Addition of dopants can accelerate reorientation in some ice phases, for example, the (partial) phase transition of hydrogen disordered hexagonal ice (ice Ih) into hydrogen ordered ice XI is possible with hydroxide as dopant, whereas acid dopants have little effect.[1–4]

We recently reported that hydrogen disordered ices V and XII transform on acid doping with HCl (DCl) into new hydrogen ordered phases, whose structures were determined by powder neutron diffraction, whereas doping with potassium hydroxide (KOH) had little effect.[5] These new ice structures were labelled ice XIII for ordered ice V, and ice XIV for ordered ice XII. The space group symmetry of hydrogen disordered ice V is $A2/a$; the monoclinic unit cell contains 28 water molecules,[6–8] and partial ordering of the water molecules is allowed by this space group. Reduction of the space group symmetry occurs on phase transition from ice V to ice XIII, from $A2/a$ to $P2_1/a$.[5] Like ice V, it comprises 28 water molecules. However, as a consequence of the reduction of space group symmetry, the number of distinct water molecules increases from four in ice V to seven in ordered ice XIII. This makes the ice XIII structure even more complicated than that of ice V and, thus, the most complicated structure among the known crystalline phases of ice.

The remarkable effect of HCl (DCl) doping on the reorientation dynamics of the two high-pressure ices came as a surprise, and it demonstrates that we know very little about the types of extrinsic defects and also the mechanism important for accelerating reorientation in the various disordered phases of ice. These results suggest a way forward in trying to clarify the mechanisms involved. The use of HCl doping represents a major step forward in releasing the geometrical frustration that locks in disorder in hydrogen bonded systems, and opens up the possibility of finally completing the phase diagram of ice.

Here we report the Raman spectra of hydrogen ordered H_2O (D_2O) ice XIII and further show that the phase transition between disordered ice V and ordered ice XIII is reversible *in vacuo*. Under these conditions, ice V and ice XIII are metastable, and this is, to our knowledge, the first reported example of a reversible phase transition between two metastable ice polymorphs. Thus, molecular reorientation has been accelerated sufficiently by the dopant to enable the phase transition at low temperatures, below the temperature of irreversible formation of cubic ice Ic. We further report the effect of various acid and alkaline dopants on hydrogen ordering in ice V and discuss the possible ordering mechanism.

Experimental

Doped ice V samples were prepared from solutions containing 0.01 M HCl (DCl) in H_2O (D_2O). For Raman spectroscopy, 5 wt% D_2O (H_2O) was added to the initial H_2O (D_2O) solution. The solutions were frozen in a piston-cylinder apparatus precooled to 77 K, and the frozen ice heated isobarically at 0.5 GPa to 250 K (*cf.* Fig. 1 in ref. 5, and ref. 9 for further

[a] *Institute of General, Inorganic and Theoretical Chemistry, University of Innsbruck, A-6020 Innsbruck, Austria. E-mail: christoph.salzmann@chem.ox.ac.uk*
[b] *Inorganic Chemistry Laboratory, University of Oxford, South Parks Road, Oxford, UK OX1 3QR. E-mail: christoph.salzmann@chem.ox.ac.uk*
[c] *Department of Physics and Astronomy, University College London, Gower Street, London, UK WC1E 6BT*

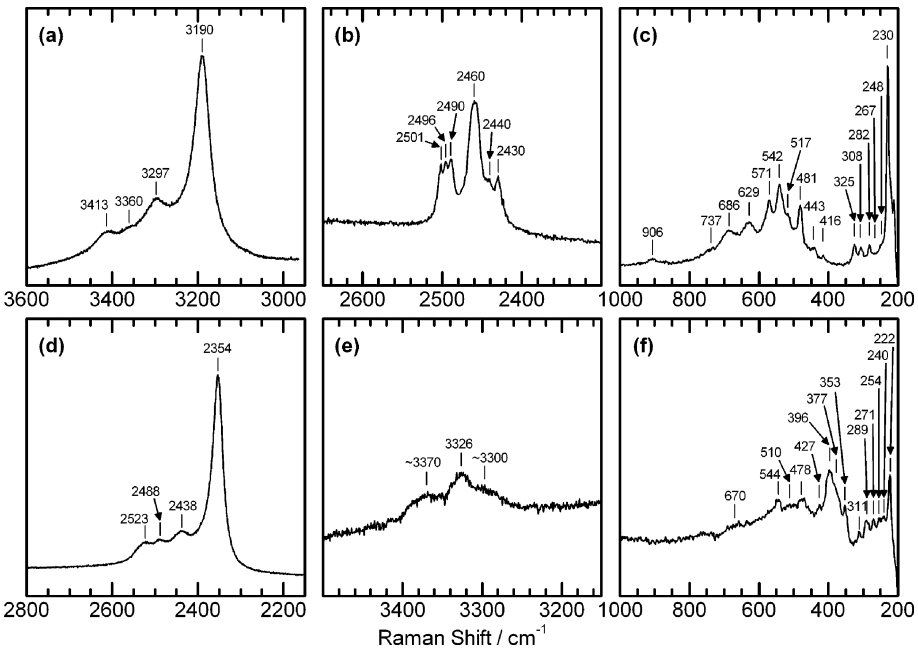

Fig. 1 Raman spectra of recovered ordered ice XIII recorded at 80 K at $\sim$10 mbar. The top frames show three spectral regions of H_2O ice XIII containing 9.0 mol% HOD, and the lower frames show the corresponding spectral regions of D_2O ice XIII containing 11 mol% HOD (see text for details).

experimental details). Thereafter, the samples were cooled from 250 K at 0.8 K min^{-1} to 77 K, decompressed, and recovered under liquid nitrogen. The transition to ice II on cooling at 0.5 GPa was never observed, which is in agreement with ref. 8. Raman spectra were recorded on a Labram-1B spectrometer equipped with a microscope (from Dilor), through a ULWD-50 objective (Olympus), by adding together four sets of spectra with an overall recording time of $\sim$10 min. A 20 mW He–Ne laser operating at 632.8 nm was used, and the 1800 L mm^{-1} grating provides a resolution of 1.1 cm^{-1} at 150 cm^{-1} increasing to 0.6 cm^{-1} at 3600 cm^{-1}. The abscissa was calibrated with a silicon standard, and the sharp Raman shifts are accurate to $\pm$2 cm^{-1}. Relative intensities of bands in different parts of the figures are not shown on the same scale. An Oxford Microstat was used as cryostat. The temperature of the sample was controlled by a LakeShore CI330 autotuning temperature controller and remained constant to within $\pm$0.2 K.

Results and discussion

Raman spectra of ice XIII

Fig. 1 shows three spectral regions of the Raman spectra of recovered ordered H_2O ice XIII containing 9.0 mol% HOD (top), and of recovered ordered D_2O ice XIII containing 11 mol% HOD (bottom). These HOD concentrations were obtained by adding 5.0 wt% D_2O (H_2O) to H_2O (D_2O). The spectra were recorded at 80 K and $\sim$10 mbar. Spectra (a) and (d) show the coupled O–H (O–D) stretching transition region with the peak maximum at 3190 (2354) cm^{-1}. Spectra (b) and (e) show the decoupled O–D (O–H) stretching transitions. Spectra (c) and (f) show the low-frequency region containing the librational and translational modes. The peak frequencies are listed in Table 1. We note that in the decoupled O–H stretching transition region ((e) and Table 1) only 3 distinct bands are observable, whereas the decoupled O–D stretching transition region (b) contains 6 distinct bands. This difference is caused partly by the poor signal-to-noise (S/N) ratio in spectrum (e), because high S/N ratio is required for resolution of strongly overlapping bands.[10] Thus, the three overlapping bands centered in (b) at 2501, 2496 and 2490 cm^{-1} become, in (e), one broad, unresolved band centered at $\sim$3370 cm^{-1}. In addition, for hydrogen ordered ice II it has been observed that the decoupled O–D stretching bands are better resolved than the decoupled O–H bands, indicating that the ratio of the full width at half heights (fwhh) of the components of the decoupled O–H and O–D bands is greater than the ratios of the peak separations.[11] A similar argument could be made here with respect to the difference in resolution between Fig. 1(b) and 1(e).

Reversible phase transition and assignment

In Fig. 2, we show the reversible phase transition of hydrogen ordered ice XIII to hydrogen disordered ice V as seen in the Raman spectra of recovered ordered H_2O ice XIII containing 9.0 mol% HOD. The spectra were recorded at the indicated temperatures and a pressure of $\sim$10 mbar. Three spectral regions are shown: (a) the coupled O–H stretching region; (b) the decoupled O–D stretching region; and (c) the region containing the librational and translational modes. Starting from the bottom, the spectrum of recovered ordered ice XIII is shown first, with the spectral features depicted in Fig. 1 (top). Thereafter, the sample was heated in steps of 10 degrees at $\sim$3 K min^{-1} and kept at each temperature for 3 min for thermal equilibration before recording the spectrum. On heating from 80 K to 120 K, pronounced changes occur in regions (b) and

Table 1 Peak frequencies of the Raman spectra of ordered H_2O (D_2O) ice XIII containing 9.0 (11) mol% HOD

H_2O peak frequencies/cm^{-1}	D_2O peak frequencies/cm^{-1}	H_2O/D_2O ratio	Assignment
3413	2523	1.35	—[a]
3360	2488	1.35	—[a]
3297	2438	1.35	—[a]
3190	2354	1.36	—[a]
—	2501	—	—[b]
~3370	2496	1.35	—[b]
—	2490	—	—[b]
3326	2460	1.35	—[b]
—	2440	—	—[b]
~3300	2430	1.36	—[b]
906	670	1.35	—[c]
737	544	1.35	—[c]
686	510	1.35	—[c]
629	478	1.32	—[c]
571	427	1.34	—[c]
542	396	1.37	—[c]
517	377	1.37	—[c]
481	353	1.36	—[c]
443	—	—	—[c]?
416	—	—	—[c]?
325	311	1.05	—[d]
308	289	1.07	—[d]
282	271	1.04	—[d]
267	254	1.05	—[d]
248	240	1.03	—[d]
230	222	1.04	—[d]

[a] The coupled O–H and O–D stretching vibrations. [b] The decoupled O–H and O–D stretching vibrations. [c] Librational modes. [d] Translational modes.

(c): the sharp bands disappear and broad unstructured bands form instead. The spectrum recorded after heating to 120 K is that of hydrogen disordered ice V (ref. 12,13 and curves 6 in Fig. 3); the decoupled O–D stretching region consists of a broad peak centred at ~2460 cm^{-1} and a shoulder ~35 cm^{-1} higher in frequency. Subsequently, the sample was cooled slowly from 120 K to 80 K at 1 K min^{-1} (*cf.* lower arrow). The spectrum recorded at 80 K is that of ordered ice XIII, and it demonstrates the reversibility of the ice XIII ↔ ice V phase transition, a result that is consistent with our previous study by powder neutron diffraction.[5]

When the sample was cooled rapidly from 120 K to 80 K at ~80 K min^{-1} (*cf.* upper arrow), then the spectrum recorded at 80 K is much less resolved in regions (b) and (c) than that of ordered ice XIII, but is much more structured than that of disordered ice V. We interpret the spectrum recorded after quenching at ~80 K min^{-1} and the splitting of bands in the spectral regions (b) and (c) as indicating that, even on quenching, the phase transition to ordered ice XIII had occurred but that this ice XIII is less ordered than that obtained on slow cooling at 1 K min^{-1}. On further heating from 130 K to 150 K, the irreversible phase transition to cubic ice Ic is seen.

Assignment of the Raman bands of ordered ice XIII to the mode-type is made by considering the H_2O/D_2O ratios of peak frequencies (*cf.* Table 1). For motions determined primarily by the hydrogen or deuterium nuclei, these ratios are close to $\sqrt{2}$.[14–16] These motions are the coupled O–H (O–D) stretching vibrations ((*a*) in Table 1), the decoupled O–H (O–D) stretching vibrations (*b*), and the librational modes (*c*). Translational modes (*d*), however, involve the motion of the whole water molecule, and consequently the ratio of H_2O:D_2O peak frequencies are close to the square root of molecular masses, $\sqrt{(20:18)}$ (= 1.05).[16]

The peak separation and resolution of bands in the decoupled O–D stretching region (Fig. 1(b)) is consistent with hydrogen (deuterium) ordering in the ice XIII phase. The fwhh of a decoupled O–D stretching transition in the IR spectrum of hydrogen ordered H_2O ice II is only ~5 cm^{-1}, but it is ~30 cm^{-1} in disordered ice I.[11,16–18] This had been attributed by Bertie and Whalley[11] to disorder in the positions of the oxygen

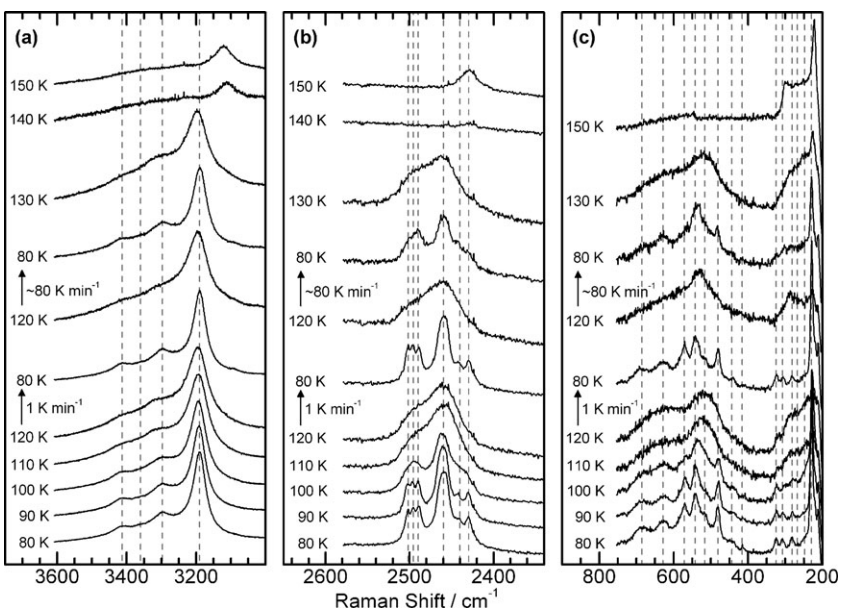

Fig. 2 The reversible ice V ↔ ice XIII phase transition as seen in the Raman spectra of recovered H_2O ice XIII containing 9.0 mol% HOD (see text for details).

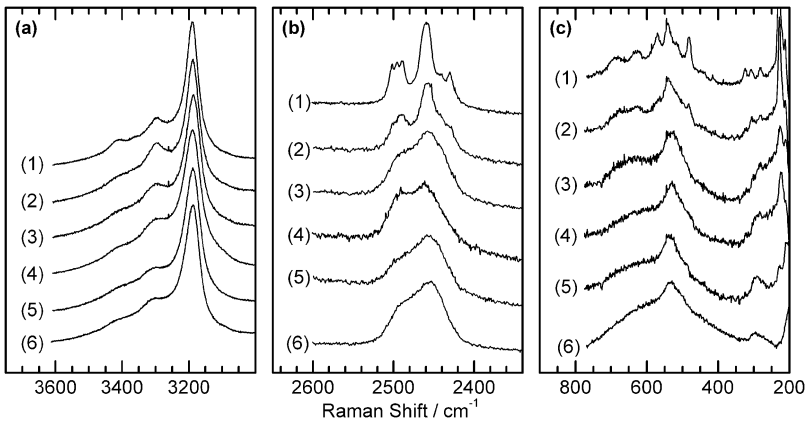

Fig. 3 Effect of dopant and of cooling rate on the Raman spectra of recovered H_2O ice V/H_2O ice XIII containing 9.0 mol% HOD and recorded at 80 K and $\sim$10 mbar (see text for details).

atoms in ice I, which was subsequently confirmed in neutron diffraction studies by Kuhs and Lehmann (reviewed in ref. 19). In Fig. 1(b), the three peaks centered at 2490, 2496 and 2501 cm^{-1} are 5–6 cm^{-1} apart and they seem to have similar intensity and band shape. For overlapping bands of Lorentzian or Gaussian band shape, separation of peak maxima must be similar to or larger than the average fwhh for resolving the distinct peak maxima (*cf*. Fig. 7 and 8 in ref. 20). Thus, the fwhh of these peaks can be at most $\sim$5–6 cm^{-1}, which is the value characteristic for an ordered ice phase. Since we compare here peak separations of the decoupled O–D stretching transition in the Raman spectrum of ice XIII (Fig. 1(b)) with those in the IR spectrum of ice II (ref. 11,16–18), the justification for this comparison must be discussed. It is well known that IR and Raman bands generally have different band shapes and widths, and Scherer[21] discusses in his review the various contributing effects. He further notes that "a major point for making these comparisons is to emphasize that very little is known about the band shape expected from a hydrogen-bonded species". Here, it is very helpful that Minceva-Sukarova *et al*.[18] compare, in their Fig. 1, the Raman spectrum of the decoupled O–D stretching transition of ice II with the IR spectrum of the same spectral region. Peak separation of the four components is about the same in the IR and Raman spectrum, which indicates similar band widths (*cf*. Table 1 in ref. 18). We conclude that the comparison of our Raman spectrum with an IR spectrum seems justified. Furthermore, hydrogen ordering does sharpen up features in the lattice vibration spectrum,[1,22] and this is what we observe here (Fig. 2).

As a consequence of the reduction of the space group symmetry from $A2/a$ to $P2_1/a$, the number of distinct water molecules *increases* from four in ice V to seven in the $P2_1/a$ phase. The number of non-equivalent O–D$\cdots$O distances thereby *increases* from 8 to 14. These 14 non-equivalent distances could be correlated with the six experimentally observed decoupled O–D stretching transitions (Fig. 1b and Table 1) by using one of the several decoupled O–D peak frequency *versus* O–D$\cdots$O bond length relations (*e.g*. ref. 23), in the same manner as reported for ice II.[11,17,18] However, this task is much more demanding for ice XIII than for ice II because the latter contains only 4 non-equivalent O–D$\cdots$O distances.[24] Furthermore, Knuts *et al*.[25] have shown, in their *ab initio* study of the OH stretching frequencies in the ordered ice phases, that the assignment of an observed decoupled stretching frequency to a particular OH bond in the structure is ambiguous when several structurally non-equivalent OH bonds are present, and their calculations suggest a reassignment of two of the experimental decoupled OD bands in ice II. Ice XIII contains highly strained four-membered rings, in addition to higher-membered rings, and thus a simple correlation of peak frequencies with O–D$\cdots$O distances is expected to be problematic. Because of this, we will refrain here from trying to make such a correlation and we will attempt it only after performing an *ab initio* study analogous to that in ref. 25.

The coupled O–H stretching band region of hydrogen ordered ice XIII seems surprisingly similar to that of hydrogen disordered ice V (*cf*. Fig. 2a for comparison), in that in this spectral region, sharp peaks do not appear on hydrogen ordering, in contrast to the spectral regions shown in Fig. 2b and 2c. Whalley[26] had already pointed out, in his classic paper on "a detailed assignment of the O–H stretching bands of ice I", the similarity of the spectra of hydrogen ordered ice VIII and disordered ice VII for this spectral region. The intense Raman band centered at 3190 cm^{-1} (Fig. 1a) can be assigned to intermolecularly coupled ν_1 vibrations of water molecules vibrating largely in phase with one another.[26] The two weak Raman bands at higher frequency are probably the asymmetric ν_3 vibrations of the water molecules split by Transverse Optic–Longitudinal Optic (TO–LO) splitting,[26] however, IR spectra are required for a definitive assignment. Whalley[26] had noted that "the similarity of the spectra of ice VII and VIII indicates that the vibrations of ice VII retain a good deal of the ν_1 or ν_3 character that they had in ice VIII", and had suggested that "the Raman spectra of orientationally ordered and disordered ice Ic (cubic ice) should also be similar to one another". Furthermore, disordered ice V can accommodate a considerable amount of hydrogen ordering within its phase, and from the neutron powder diffraction study by Lobban *et al*.,[8] up to 45% ordering occurs for undoped D_2O ice V recovered at 101.8 K (calculated from Table 3 in ref. 8). Differences do exist between the Raman spectra of ordered

ice XIII and disordered ice V in the coupled O–H stretching band region. Firstly, the band width of the intense band centered at 3190 cm^{-1} is smaller for ice XIII than ice V, as expected as an effect of hydrogen ordering (48 cm^{-1} for ice XIII at 80 K (bottom spectrum in Fig. 2(a)) and 57 cm^{-1} for ice V at 80 K (bottom spectrum in Fig. 3(a)). Secondly, the two weak Raman bands centered at 3297 and 3413 cm^{-1} are much more intense and sharper in the spectrum of ice XIII than that of ice V.

Comparison of dopants

We next show the effect of the type of dopant, and of cooling rate under pressure, on the Raman spectra of recovered H_2O ice V/H_2O ice XIII containing 9.0 mol% HOD. The samples were prepared from solutions containing 0.01 M of the dopant in H_2O, and 5 wt% of D_2O. First, doped ice V was made as described above, by freezing the solutions in a piston-cylinder apparatus precooled to 77 K, and then heating the frozen ice isobarically at 0.5 GPa to 250 K. Thereafter, ice V containing the dopant was cooled at 0.5 GPa either slowly from 250 K to 77 K, or quenched at a rate of 40 K min^{-1}. Fig. 3 shows Raman spectra of the samples recovered at 77 K and recorded at 80 K for the three spectral regions containing (a) the coupled O–H stretching transitions, (b) the decoupled O–D stretching transitions, and (c) the librational and translational modes. Curves (1) are from a sample of HCl doped ice V which was slowly cooled at 0.5 GPa from 250 K to 77 K at 0.8 K min^{-1}. The spectral features are those of fully ordered ice XIII (compare with Fig. 1, top). Curves (2) are from a new sample of HCl doped ice V that was quenched at 0.5 GPa and a rate of 40 K min^{-1} from 250 K to 77 K. The spectral features in the regions (b) and (c) are much less resolved than those in curves (1), and they resemble those shown in Fig. 2 after quenching from 120 K to 80 K at a rate of $\sim$80 K min^{-1} (*cf.* upper arrow).

Curves (3) in Fig. 3 are from a sample of HF doped ice V that was slowly cooled at 0.5 GPa from 250 K to 77 K at 0.4 K min^{-1}, and curves (4) are from a new sample of HF doped ice V quenched to 77 K at $\sim$40 K min^{-1}. Curves (5) are from a sample of KOH doped ice V that was slowly cooled at 0.5 GPa from 250 K to 77 K at 0.4 K min^{-1}. Curves (6) show, for comparison, the spectral features of undoped ice V which was slowly cooled at 0.5 GPa from 250 to 77 K at 0.4 K min^{-1}. Curves (3) to (5) differ from curves (1) and (2), in particular in the decoupled O–D stretching transition region (b), where a broad band centred at $\sim$2457 cm^{-1} is observed with a more or less pronounced shoulder at higher frequency. These are the spectral features reported for undoped ice V,[12,13] shown for comparison in curves (6). We conclude that HF and KOH doping of ice V (curves (3) to (5)) does not induce sufficient orientational ordering to cause a phase transition to ordered ice XIII. Minor differences between the spectral features of curves (3) to (5) could be attributed to varying amounts of orientational ordering within the ice V phase.[8] In particular, in curve (4) of Fig. 3(b), enhanced intensity of the shoulder at high frequency of the decoupled O–D stretching transition is observed. This feature was found to be reproducible in a new sample, but it is not easily interpreted.

Discussion of HCl dopant

The effect of the cooling rate on isobaric cooling at 0.5 GPa on the Raman spectral features of HCl doped recovered samples (curves (1) and (2) in Fig. 3) is comparable to that on cooling *in vacuo* (*cf.* Fig. 2), and it reflects the relaxation time of hydrogen ordering in the ice V $\rightarrow$ ice XIII phase transition and its temperature dependence. Lobban *et al.*[8] have reported, in a neutron powder diffraction study at 0.5 GPa, increasing orientational ordering in D_2O ice V with decreasing temperature. They concluded from a consideration of the orientational ordering and the cooling rate that the relaxation time at 125 K could possibly be around 100 s, and at 100 K, $\sim$3000 s (Fig. 6 in ref. 8) These estimates were obtained for undoped D_2O ice V samples. For our samples of H_2O (D_2O) ice V doped with HCl (DCl), they must be much shorter. We will give estimates of relaxation times in a forthcoming detailed publication reporting neutron powder diffraction studies of HCl doped samples, and then attempt to relate the degree of orientational ordering to the cooling rate. We note that Johari and Whalley[27] have studied the dielectric relaxation spectra of ice V over the 133–270 K range, and calculated a dielectric relaxation time value of 1.5 s at 133 K. Extrapolation to lower temperatures, *e.g.* to 100 K, is not meaningful because they argue that below 133 K, the Arrhenius plot of τ *vs.* $1/T$ might not be linear because of a possible increase of activation energy (*cf.* their Fig. 4C, region III).

We now discuss the remarkable effect of HCl as dopant in accelerating the reorientation of water molecules and hydrogen (deuterium) ordering at low temperatures. At high temperatures, water ices can explore their configurational manifold thanks to the presence of mobile point defects that locally lift the geometrical frustration constraints.[1,5,8,28] The two types of thermally-induced point defects uniquely found in ices are (a) rotational defects in which either two (D defect) or no (L defect) hydrogen atoms are found between neighbouring oxygen atoms, and (b) ionic defects (H_3O^+ and OH^-) (*cf.* ref. 1 and 5 for discussion). With decreasing temperature, reorientational ordering of water molecules is hampered by the decreasing number and mobility of these point defects. Except for disordered ices III and VII, intrinsic point defects are not sufficient to facilitate phase transitions from the hydrogen disordered phases to their hydrogen ordered phases. Extrinsic point defects can also be introduced by doping ices with impurities, such as in the partial conversion of hydrogen disordered ice Ih to hydrogen ordered ice XI facilitated by KOH doping.[1–4] KOH doping is expected to generate L and OH^- defects, whereas HCl doping is thought to produce L and H_3O^+ defects.[1] Thus, the remarkable effect of HCl doping in comparison to that of doping with KOH (*cf.* Fig. 3) seems to be caused by H_3O^+ defects. The minor effect of HF doping (*cf.* Fig. 3 curves (3) and (4)) thus might be due to the weaker acid strength of HF in comparison to that of HCl, and the reduced number of H_3O^+ defects. It is interesting to note that HF, which is one of the most soluble and active dopants for ice Ih,[1] does not cause hydrogen ordering in ice V in the way HCl does.

The maximum solubility of HCl in ice Ih at *e.g.* 263 K is 3×10^{-6} mole fraction, [1,29] and thus the HCl concentration in the

0.01 M HCl solution used in our studies is higher than this by about two orders of magnitude. Therefore, HCl is expected to be present in ice Ih after quenching to 77 K as a mixture of "solid solution + aqueous solution" (*cf*. Fig. 1 in ref. 29). The solubility of HCl can change in an unknown manner once ice V is formed. Also, the number density and mobility of extrinsic point defects caused in ice V by the HCl dopant is unknown. We observed that, according to calorimetry, 0.001 M HCl has a similar effect on hydrogen ordering in ice V as does 0.01 M HCl (to be reported separately). In conclusion, it seems likely that the HCl dopant acts purely as a catalyst of this hydrogen disorder–order transformation.

The effect of KOH doping on hydrogen ordering in ice V has been studied by heat-flow calorimetry[30] and by Raman spectroscopy.[31] Handa *et al*.[30] observed, in their calorimetric study of undoped and KOH doped ice V, an endothermic peak between 105–140 K whose size increased with KOH doping and annealing time. They concluded that the endotherm indicates an order–disorder phase transition. However, Raman spectroscopic studies of undoped ice V and of KOH doped ice V by Minceva-Sukarova *et al*.[31,32] could not confirm a phase transition. In these Raman studies spectroscopic evidence for partial proton ordering below $\sim$130 K was observed in the lattice vibration region of undoped ice V,[32] and in the decoupled O–D stretching transition region of KOH doped ice V.[31] They concluded that "some kind of proton ordering or partial proton ordering may be induced by the presence of KOH dopant",[31] but they also noted that "infrared and Raman spectroscopy is not as sensitive as other techniques in detecting ordering". Our comparison of the Raman spectra of HCl doped ice V (Fig. 3, curves 1) with those of KOH doped ice V (Fig. 3, curves 5) clearly shows that the phase transition requires HCl rather than KOH doping. Thus, the previous evidence for partial hydrogen ordering in undoped ice V,[8,30,32,33] or in KOH doped ice V[30,31] must have been obtained within the ice V phase, which allows considerable hydrogen ordering.[6–8]

Acknowledgements

We thank the "Forschungsförderungsfonds" of Austria (project No. P13930-PHY) and the University of Innsbruck (C.G.S.) for financial support.

References

1 V. F. Petrenko and R. W. Whitworth, *'Physics of Ice'*, Oxford University Press, 1999.
2 Y. Tajima, T. Matsuo and H. Suga, *Nature*, 1982, **299**, 810.
3 Y. Tajima, T. Matsuo and H. Suga, *J. Phys. Chem. Solids*, 1984, **45**, 1135.
4 H. Suga, *Pure Appl. Chem*., 1983, **55**, 427.
5 C. G. Salzmann, P. G. Radaelli, A. Hallbrucker, E. Mayer and J. L. Finney, *Science*, 2006, **311**, 1758.
6 W. C. Hamilton, B. Kamb, S. J. La Placa and A. Prakash, ed. B. B. N. Riehl and H. Engelhardt, New York, 1969.
7 W. F. Kuhs, C. Lobban and J. L. Finney, *Rev. High Pressure Sci. Technol*., 1998, **7**, 1141.
8 C. Lobban, J. L. Finney and W. F. Kuhs, *J. Chem. Phys*., 2000, **112**, 7169.
9 C. G. Salzmann, I. Kohl, T. Loerting, E. Mayer and A. Hallbrucker, *J. Phys. Chem. B*, 2003, **107**, 2802.
10 P. Gans and J. B. Gill, *Anal. Chem*., 1980, **52**, 351.
11 J. E. Bertie and E. Whalley, *J. Chem. Phys*., 1964, **40**, 1646.
12 M. J. Taylor and E. Whalley, *J. Chem. Phys*., 1964, **40**, 1660.
13 B. Minceva-Sukarova, W. F. Sherman and G. R. Wilkinson, *J. Phys. C: Solid State Phys*., 1984, **17**, 5833.
14 C. Haas and D. F. Hornig, *J. Chem. Phys*., 1960, **32**, 1763.
15 J. E. Bertie and E. Whalley, *J. Chem. Phys*., 1964, **40**, 1637.
16 D. Eisenberg and W. Kauzmann, *The Structure and Properties of Water*, Oxford University Press, 1969.
17 J. E. Bertie and F. E. Bates, *J. Chem. Phys*., 1977, **67**, 1511.
18 B. Minceva-Sukarova, W. F. Sherman and G. R. Wilkinson, *Spectrochim. Acta, Part A*, 1985, **41**, 315.
19 W. F. Kuhs and M. S. Lehmann, in *'The Structure of Ice-Ih'*, ed. F. Franks, Cambridge, 1986.
20 G. Fleissner, W. Hage, A. Hallbrucker and E. Mayer, *Appl. Spectrosc*., 1996, **50**, 1235.
21 J. R. Scherer, in *'The Vibrational Spectroscopy of Water'*, ed. R. J. H. Clark and R. E. Hester, London, 1978.
22 B. Minceva-Sukarova, G. E. Slark, W. F. Sherman and G. R. Wilkinson, *J. Phys*., 1987, **48**, C1.
23 C. A. Tulk, D. D. Klug, R. Branderhorst, P. Sharpe and J. A. Ripmeester, *J. Chem. Phys*., 1998, **109**, 8478.
24 B. Kamb, W. C. Hamilton, S. J. LaPlaca and A. Prakash, *J. Chem. Phys*., 1971, **55**, 1934.
25 S. Knuts, L. Ojamäe and K. Hermansson, *J. Chem. Phys*., 1993, **99**, 2917.
26 E. Whalley, *Can. J. Chem*., 1977, **55**, 3429.
27 G. P. Johari and E. Whalley, *J. Chem. Phys*., 2001, **115**, 3274.
28 G. P. Johari, *Chem. Phys*., 2000, **258**, 277.
29 E. Thibert and F. Domine, *J. Phys. Chem. B*, 1997, **101**, 3554.
30 Y. P. Handa, D. D. Klug and E. Whalley, *J. Phys. Colloq*., 1987, **48**, 435.
31 B. Minceva-Sukarova, G. Slark and W. F. Sherman, *J. Mol. Struct*., 1988, **175**, 289.
32 B. Minceva-Sukarova, G. E. Slark and W. F. Sherman, *J. Mol. Struct*., 1986, **143**, 87.
33 C. G. Salzmann, I. Kohl, T. Loerting, E. Mayer and A. Hallbrucker, *Phys. Chem. Chem. Phys*., 2003, **5**, 3507.